

Thermal stability of magnetic nanostructures in ion-bombardment-modified exchange-bias systems

V. Höink,* M. D. Sacher, J. Schmalhorst, and G. Reiss

Thin Films and Nanostructures, Department of Physics, University of Bielefeld, P.O. Box 100131, 33501 Bielefeld, Germany

D. Engel, T. Weis, and A. Ehresmann

Institute of Physics and Center for Interdisciplinary Nanostructure Science and Technology (CINSA^T), Kassel University, Heinrich-Plett-Str.40, D-34132 Kassel, Germany

(Received 22 February 2006; published 20 June 2006)

In magnetic bilayer systems consisting of a ferromagnet and an antiferromagnet the strength and direction of the exchange bias coupling can be set by ion bombardment in an external magnetic field. Magnetic nanostructures with a laterally varying exchange bias direction can be produced by local ion bombardment (ion bombardment induced magnetic patterning). We have investigated the thermal stability of these magnetic nanostructures by *in situ* x-ray photoemission electron microscopy while heating the samples above their blocking temperature. The investigations have been done at a $10.4\ \mu\text{m} \times 10.4\ \mu\text{m}$ large checkered pattern with a minimum size of the magnetic patterns of $800\ \text{nm} \times 800\ \text{nm}$ on a field cooled MnIr/CoFe stack and a pattern with $1.6\ \mu\text{m}$ wide lines with a periodicity of $5\ \mu\text{m}$ on an as-prepared MnIr/Co stack. The temperature dependence of the magnetization pattern can be explained by the temperature dependence of the exchange bias interaction, the exchange interaction energy, and the stray field energy. No substantial change of the thermal stability of magnetic patterns in remanence by the ion bombardment was found.

DOI: [10.1103/PhysRevB.73.224428](https://doi.org/10.1103/PhysRevB.73.224428)

PACS number(s): 75.75.+a, 75.70.Cn, 61.80.Jh, 68.37.Yz

I. INTRODUCTION

When a ferromagnetic layer (FM) is in contact with an antiferromagnetic layer (AFM) a shift of the FM hysteresis loop due to the exchange coupling at the FM/AFM interface can occur. This effect is called exchange bias (EB).¹ Possible procedures to initialize or change the EB in polycrystalline layer systems are, e.g., field cooling (FC: annealing and subsequent cooling in a magnetic field with a maximum temperature above the blocking temperature T_B , but below the Curie temperature T_C of the FM) or bombardment of the sample with light ions (e.g., He) in an external magnetic field (IB). With IB the exchange bias can be initialized or changed in sign and size.²⁻⁵ In contrast to FC, which always results in a homogenous unidirectional anisotropy in the whole bilayer, IB makes it possible to choose the area in which the unidirectional anisotropy is manipulated by restricting the bombarded area (ion bombardment induced magnetic patterning, IBMP). For small external fields this patterned EB coupling results in a corresponding arrangement of the magnetization of the pinned FM. For the application of this lateral magnetic patterning in, e.g., giant magnetoresistance (GMR) (Ref. 6) or magnetic tunnel junction (MTJ) (Ref. 7) devices the AFM/FM-bilayer acts as a magnetic reference layer where it is important that the FM magnetization is stable. For an application in a hot environment as, e.g., in the automotive industry, temperature stability can be a limiting factor. It is known, that the exchange bias vanishes above the blocking temperature T_B (Ref. 1) limiting the thermal stability of every EB coupled layer system to this temperature. Here we present x-ray photoemission electron microscopy (PEEM) measurements showing how and at which temperature a magnetic pattern produced by IB on a typical reference electrode of a magnetic tunnel junction (MTJ) is changed by

successive heating. This investigation shows that the choice of IB for the manipulation of the EB does not influence the thermal stability in remanence and therefore does not limit the applicability of the magnetic pattern.

II. EXPERIMENT

Two different magnetic layer systems were prepared by dc and rf magnetron sputtering on thermally oxidized silicon wafers at room temperature (RT). The layer stack A is Cu 30 nm/Mn₈₃Ir₁₇ 15 nm/Co₇₀Fe₃₀ 3 nm/Al 1.4 nm +100 s electron cyclotron resonance (ECR) plasma oxidation with $-10\ \text{V}$ bias voltage,⁸ and corresponds to the lower part of a typical MTJ.⁹ The Cu layer is the lower conduction line. The CoFe (FM), which is pinned by the adjacent MnIr (AFM), is used as the reference electrode of the MTJ. In this experiment the 1.8 nm thick Al-oxide tunnel barrier serves as an oxidation preventing capping layer. Sample A was annealed for 1 h at 548 K in an external magnetic field of $H_{\text{FC}}=1\ \text{kOe}$. Sample B has a similar stack with the ferromagnet Co and an additional NiFe seed layer: Cu 30 nm/Ni₈₀Fe₂₀ 1.9 nm/Mn₈₃Ir₁₇ 25 nm/Co 3 nm/Al 1.4 nm+100 s oxidation. No FC was carried out for stack B. To define the area which was bombarded by ions, the samples were spin coated with an approximately 500 nm thick e-beam resist layer. Then the resist was patterned by electron beam lithography. On sample A amongst others a $10.4\ \mu\text{m} \times 10.4\ \mu\text{m}$ large checkered pattern was produced. $1.2\ \mu\text{m} \times 1.2\ \mu\text{m}$ large bombarded squares were arranged with a center to center distance of $2\ \mu\text{m}$ resulting in $0.8\ \mu\text{m} \times 0.8\ \mu\text{m}$ large quadratic not bombarded areas in between the bombarded squares. The edges of the squares have been oriented parallel/perpendicular to \mathbf{H}_{FC} . On sample B as well as on sample A $1.6\ \mu\text{m}$ wide lines with a periodicity of

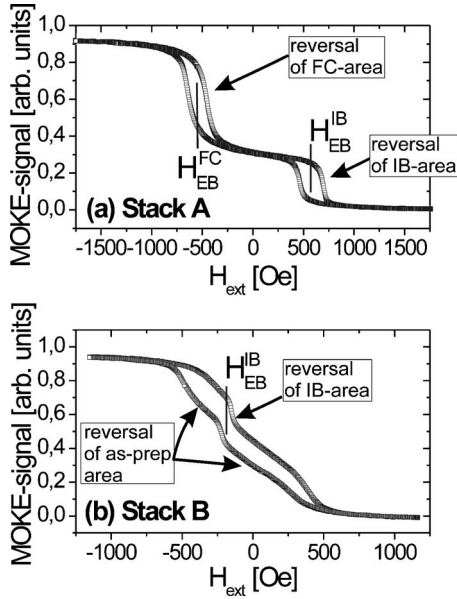


FIG. 1. MOKE measurements at RT on the magnetically patterned areas of stack A (a) and stack B (b) after IB. H_{EB}^{FC} is the EB field measured for the not bombarded but field cooled areas and H_{EB}^{IB} is the EB field measured in the bombarded areas.

5 μm were patterned. The samples were bombarded through the resist mask with He ions with an energy of 10 keV and an ion dose of 1×10^{14} ions/cm². The external magnetic field applied during IB was $H_{IB}=1$ kOe for all samples. In the case of sample A, \mathbf{H}_{IB} was oriented antiparallel to \mathbf{H}_{FC} while it was aligned parallel to the patterned lines during the bombardment of stack B. After IB the resist mask was removed and the resulting magnetic pattern were investigated at RT by magneto-optical Kerr-effect magnetometry (MOKE). PEEM measurements were carried out while heating the samples *in situ* at the PEEM-2 beamline 7.3.1.1 at the Advanced Light Source, Berkeley, CA.¹⁰ For sample A measurements were done while heating the sample from room temperature (RT) to 667 K. Sample B was measured while heating it up to 565 K and cooling it down to 348 K. All measurements were done in remanence with elliptically polarized x rays with a degree of polarization of 75%. To visualize the domain pattern of the FM, the XMCD effect¹¹ was utilized. Therefore at every investigated temperature PEEM images were taken at the Co L_3 edge and at the Co L_2 edge. The ratio of the two images was calculated to gain information of the magnetic domains. Magnetic force microscopy (MFM) measurements at RT were carried out with another identically patterned part of sample A which has not been used for the PEEM heating experiment before. Alternating gradient magnetometer (AGM) measurements were carried out at several temperatures with field cooled samples as well as with field cooled and additionally ion bombarded samples with layer stacks A and B.

III. RESULTS AND DISCUSSION

The results of the MOKE measurements on the magnetic pattern of stack A after IB can be seen in Fig. 1(a). The

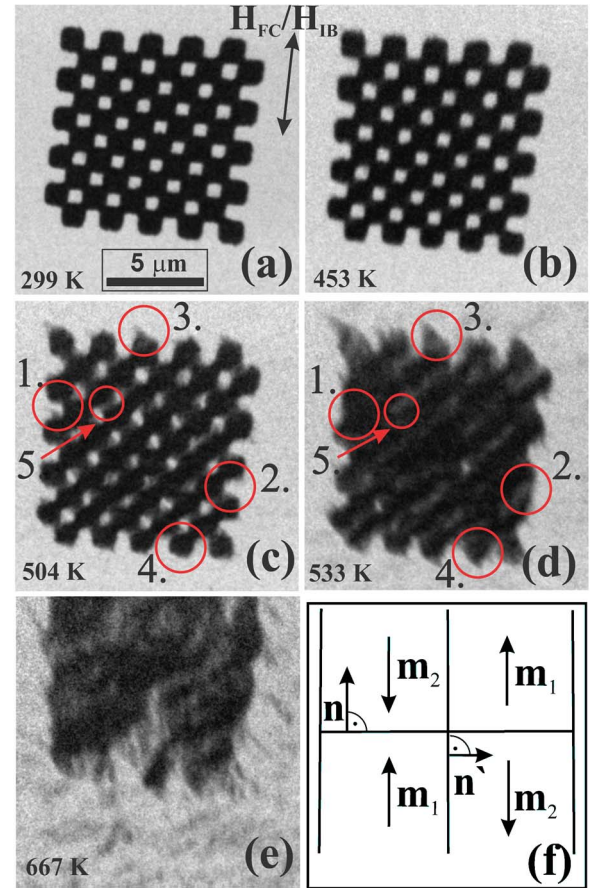


FIG. 2. (Color online) PEEM measurements of stack A (FM: CoFe, $\mathbf{H}_{IB} \uparrow \downarrow \mathbf{H}_{FC}$, magnetization $\uparrow \uparrow \mathbf{H}_{IB}$: dark, magnetization $\uparrow \uparrow \mathbf{H}_{FC}$: bright) at (a) 299 K, (b) 453 K, (c) 504 K, (d) 533 K, and (e) 667 K; (f) FM areas with different magnetization direction \mathbf{m} . The shift of the domain pattern to the upper part of the image is due to a thermal elongation of the sample holder.

external field \mathbf{H}_{ext} during the measurement was aligned (anti) parallel to $\mathbf{H}_{IB}/\mathbf{H}_{FC}$. Because the diameter of the analyzed area on the sample of ≈ 0.2 mm was larger than the single magnetic structures, a superposition of the signals originating from the bombarded and the not bombarded areas was obtained. The exchange bias field measured at the bombarded area of $\mathbf{H}_{EB}^{IB}=570$ Oe has approximately the same absolute value as measured in the field cooled area ($\mathbf{H}_{EB}^{FC}=-550$ Oe) but of the opposite sign. These values are comparable to earlier results measured for the combination MnIr/CoFe in MTJs.⁹ Figure 1(b) shows a magnetization loop measured by MOKE on a magnetically patterned area of sample B (FM: Co). \mathbf{H}_{ext} was aligned (anti) parallel to \mathbf{H}_{IB} . The curve shows again a superposition of the signals originating from the bombarded and the not bombarded area. The exchange bias field measured at the bombarded area is $H_{EB}^{IB}=190$ Oe. This value also is comparable to former results.¹² The shape of the signal of the as-prepared part can be explained by a local pinning of the Co to the MnIr with randomly distributed directions of the easy axis.

Figure 2 shows selected PEEM images of sample A. It can be seen in Fig. 2(a) (RT) that domains with the magnetization oriented parallel to \mathbf{H}_{FC} appear bright while the bom-

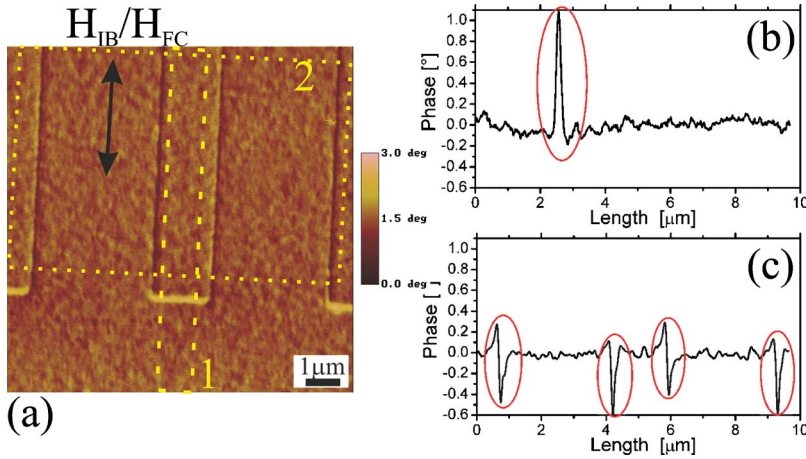


FIG. 3. (Color online) (a) MFM measurement of a second structure on stack A (bombarded lines, $\mathbf{H}_{IB} \uparrow \downarrow \mathbf{H}_{FC}$), (b) line scan parallel to lines (averaged over area 1 indicated by dashed box in MFM image; head to head orientation of magnetization: large interface charge density), (c) line scan perpendicular to lines (averaged over area 2 indicated by dotted box in the MFM image; low interface charge density); The ellipses in (b) and (c) mark the domain walls between bombarded and not bombarded areas. Different offsets have been applied to the line scans and the MFM image.

bombarded domains with an opposite direction of the magnetization appear dark in the processed PEEM images. The rounded edges originate from a corresponding shape of the resist mask. Temperatures up to 453 K do not induce a considerable change of the magnetic pattern [Fig. 2(b)]. The blocking temperature at which the exchange bias coupling vanishes after a strong decrease over a wide temperature range was determined by AGM measurements to be in the range of 495–525 K for other samples with the same layer stack. The other energy terms contributing to the total free energy do not vanish at this temperature: in Ref. 13 a temperature dependence of the exchange stiffness energy proportional to the cube of the saturation magnetization [$J_S(T)^3$] was found for FePd while a proportionality to $J_S(T)^2$ is supposed in Ref. 14. The stray field energy follows $J_S(T)^2$.¹⁵ AGM measurements at other samples with this layer stack have in all cases shown a decrease of the saturation magnetization $J_S(T)$ between RT and T_B of less than 20%. In summary one can see that while reaching the blocking temperature the influence of the latter two energy contributions grows relatively to the exchange bias coupling and therefore a degradation of the magnetic pattern in this temperature range and above can be observed. All samples were sputtered without an external field. Therefore one can expect that the FM layer does not show a macroscopic anisotropy.

Figure 2(c) shows a PEEM measurement at 504 K where a change in the domain pattern can be seen clearly. Between 453 K and 504 K bright domains begin to grow gradually into the dark ones and vice versa [Fig. 2(c)]. One striking effect is that the prolate dark domains growing into the not bombarded area around the magnetic pattern only can be observed at those edges where the magnetization direction of the dark and the bright domains are oriented head to head (see, e.g., circles 1–3). This behavior can be seen even better at the measurement shown in Fig. 2(d) (533 K). The indentations at the sides vanish [e.g., Fig. 2(d), circles 1, 2] and the domain walls which were oriented perpendicular to $\mathbf{H}_{FC}/\mathbf{H}_{IB}$ after IB (head to head orientation of the magnetization) switch to a diagonal or frayed pattern (circles 3–5). In contrast to this the corners parallel to $\mathbf{H}_{FC}/\mathbf{H}_{IB}$ on the outer sides of the magnetic pattern remain unchanged (circles 1,2). This can be explained by the influence of stray fields resulting from interfacial magnetic charges with a reduced inter-

face charge density of $\sigma = (\mathbf{m}_1 - \mathbf{m}_2) \cdot \mathbf{n}$ [Ref. 15, $\mathbf{m}(\mathbf{r}) = \mathbf{J}(\mathbf{r})/J_S$, \mathbf{n} : vector normal to pattern boundary, see Fig. 2(f)]. At the domain walls with a head to head orientation of the magnetization the vector $(\mathbf{m}_1 - \mathbf{m}_2)$ is aligned parallel to the normal vector \mathbf{n} resulting in a maximum interface charge density while at the domain walls parallel to $\mathbf{H}_{FC}/\mathbf{H}_{IB}$ ($\mathbf{m}_1 - \mathbf{m}_2$) is oriented perpendicular to \mathbf{n} . Therefore no magnetic charges occur in the latter case.

The magnetic force microscopy (MFM) measurement of bombarded lines on another field cooled part of the same sample A which is shown in Fig. 3 confirms these considerations. \mathbf{H}_{IB} was oriented parallel to the lines and antiparallel to \mathbf{H}_{FC} . Therefore the relative orientation of the magnetization at the end of the bombarded lines is head to head to the magnetization of the surrounding area. As expected this area shows the largest stray field. According to the energy minimization principle it can be expected that the energetically unfavorable “head to head” domain walls in the heated sample will be altered at high temperatures when their existence is not enforced any longer by the exchange bias interaction. Furthermore a temperature induced nucleation of dark domains can be seen in the not bombarded (bright) area at the temperature of 533 K [Fig. 2(d)]. They gain in size during the further heating up to the maximum investigated temperature of 667 K [Fig. 2(e)]. Even about 160 K above the blocking temperature the bombarded area is still visible by a darker average color in the PEEM image. This is due to an exchange length smaller than the size of the magnetic pattern. Note that the $0.8 \mu\text{m} \times 0.8 \mu\text{m}$ large bright domains in the inner part of the magnetic pattern disappeared.

The magnetic pattern on sample B (FM: Co) which was not field cooled prior to IB consists of $1.6 \mu\text{m}$ wide bombarded lines with a periodicity of $5 \mu\text{m}$. The magnetic field during IB was oriented parallel to the lines. The magnetic structure of the sample at RT with a uniform magnetization at the bombarded lines (bright) and small domains in the as prepared area can be seen at the PEEM image in Fig. 4(a). At a temperature of 389 K independent of the IB a thermally activated domain growth starts. This can be seen by comparing the marked area of the zoomed PEEM image measured on a not bombarded part of the sample at 384 K [Fig. 4(b)] with the image of the same area taken at 389 K [Fig. 4(c)] where the dark domain has grown into the bright one. A

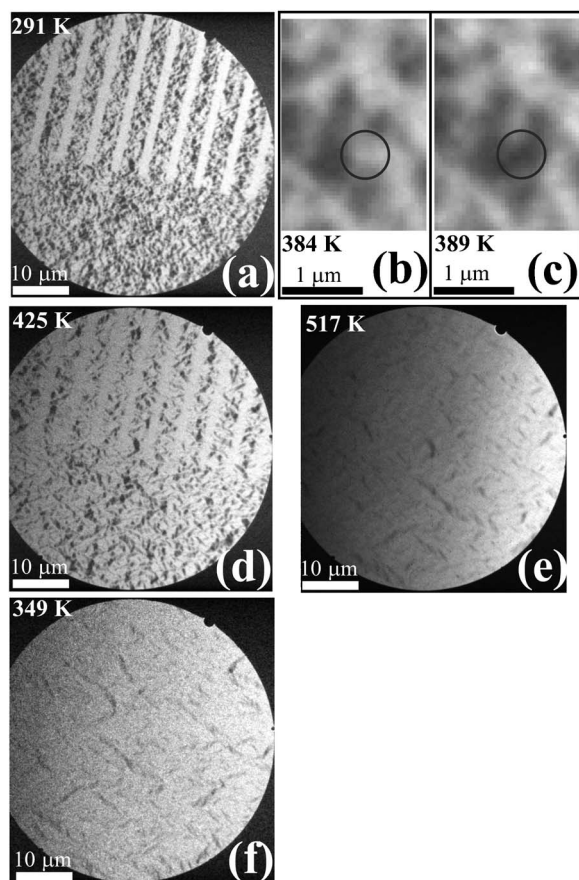


FIG. 4. PEEM measurements of stack B (FM: Co, no FC, $H_{IB} \uparrow \uparrow$ to bombarded lines) while heating at 291 K (a), 384 K (b), 389 K (c), 425 K (d), and 517 K (e) and after cooling to 349 K (f). The shift of the lines is due to a thermal elongation of the sample holder.

growth of bright domains into dark ones can be observed as well (not shown). For rising temperatures the growth of the small domains in the as prepared area continues [Fig. 4(d)]. For $T \geq 425$ K dark domains partly grow into the bombarded area, until at 517 K [Fig. 4(e)] and for higher temperature (not shown) no trace of the bombarded lines can be found. The same considerations about energy minimization as used

for stack A can be applied here again. The disappearance of the lines is due to the smaller size of the thin lines compared to the compact checked pattern on sample A. After cooling the sample to 349 K the domain state is frozen. No specific features as, e.g., different domain sizes due to a change of the microstructure of the sample by IB can be seen in the domain state of the bombarded area in comparison to the not bombarded area after the heating and cooling process.

IV. SUMMARY

We have investigated the thermal stability of the reference part of MTJs with CoFe and Co used as FM. The magnetic pattern produced by IB in an external field on the field cooled stack A (CoFe) was stable up to about 450 K and changed its shape due to the growing influence of stray fields and a reduction of the stabilizing EB energy for higher temperatures. The alteration of the magnetic pattern occurs in the range of the blocking temperature. Therefore we have no indication for a change of the thermal stability of magnetic structures in remanence due to the ion bombardment. On the as-prepared stack B (Co) first changes of the domain structure in the as-prepared area were seen at 389 K independent of the IB, while the direction of the magnetization on the bombarded area was stable up to the temperature of about 425 K. As the as-prepared area showed a domain growth at lower temperatures than the bombarded area we have again no hint that the IB decreases the thermal stability in remanence. The minimum size of the investigated magnetic structures produced by IBMP was $800 \text{ nm} \times 800 \text{ nm}$.

ACKNOWLEDGMENTS

The authors gratefully acknowledge A. Scholl and A. Doran for the assistance during the measurements at the Advanced Light Source, Berkeley. The financial support by the Deutsche Forschungsgemeinschaft DFG is also gratefully acknowledged. The Advanced Light Source is supported by the Director, Office of Science, Office of Basic Energy Sciences, Materials Sciences Division, of the U.S. Department of Energy under Contract No. DE-AC03-76SF00098 at Lawrence Berkeley National Laboratory.

*Electronic address: vhoink@physik.uni-bielefeld.de

¹J. Nogues and I. K. Schuller, *J. Magn. Magn. Mater.* **192**, 203 (1999).

²C. Chappert, H. Bernas, J. Ferre, V. Kottler, J.-P. Jamet, Y. Chen, E. Cambril, T. Devolder, F. Rousseaux, V. Mathet, and H. Launois, *Science* **280**, 1919 (1998).

³J. Fassbender, D. Ravelosona, and Y. Samson, *J. Phys. D* **37**, R179 (2004).

⁴A. Ehresmann, *Recent Res. Dev. Phys.* **7**, 401 (2004).

⁵D. Engel, A. Ehresmann, J. Schmalhorst, M. Sacher, V. Höink, and G. Reiss, *J. Magn. Magn. Mater.* **293**, 849 (2005).

⁶J. Fassbender, S. Poppe, T. Mewes, J. Juraszek, B. Hillebrands,

K.-U. Barholz, R. Mattheis, D. Engel, M. Jung, H. Schmoranzler, and A. Ehresmann, *Appl. Phys. A* **77**, 51 (2003).

⁷V. Höink, M. D. Sacher, J. Schmalhorst, G. Reiss, D. Engel, D. Junk, and A. Ehresmann, *Appl. Phys. Lett.* **86**, 152102 (2005).

⁸A. Thomas, H. Brückl, M. Sacher, J. Schmalhorst, and G. Reiss, *J. Vac. Sci. Technol. B* **21**, 2120 (2003).

⁹J. Schmalhorst, V. Höink, G. Reiss, D. Engel, D. Junk, A. Schindler, A. Ehresmann, and H. Schmoranzler, *J. Appl. Phys.* **94**, 5556 (2003).

¹⁰S. Anders, H. A. Padmore, R. M. Duarte, T. Renner, T. Stämmler, A. Scholl, M. Scheinfein, J. Stöhr, L. Stéve, and B. Sinkovic, *Rev. Sci. Instrum.* **70**, 3973 (1999).

- ¹¹J. Stöhr, *J. Electron Spectrosc. Relat. Phenom.* **75**, 253 (1995).
- ¹²J. Schmalhorst, M. Sacher, V. Höink, G. Reiss, D. Engel, and A. Ehresmann, *Phys. Rev. B* **70**, 184403 (2004).
- ¹³M. Mulazzi, K. Chesnel, A. Marty, G. Asti, M. Ghidini, M. Solzi, M. Belakhovsky, N. Jaouen, J. Tonnerre, and F. Sirotti, *J. Magn. Mater.* **272-276**, e895 (2004).
- ¹⁴A. P. Malozemoff and J. C. Slonczewski, *Magnetic Domain Walls in Bubble Materials* (Academic, New York, 1979).
- ¹⁵A. Hubert and R. Schäfer, *Magnetic Domains* (Springer-Verlag, Berlin, 1998).